β_2-Adrenergic receptor supports prolonged theta tetanus-induced LTP

Hai Qian,[1] Lucas Matt,[2] Mingxu Zhang,[1,2] Minh Nguyen,[2] Tommaso Patriarchi,[2] Olha M. Koval,[3] Mark E. Anderson,[3] Kaiwen He,[4] Hey-Kyoung Lee,[4] and Johannes W. Hell[1,2]

Departments of [1]Pharmacology and [3]Internal Medicine, University of Iowa, Iowa City, Iowa; [2]Department of Pharmacology, University of California, Davis, California; and [4]Department of Biology, University of Maryland, College Park, Maryland

Qian H, Matt L, Zhang M, Nguyen M, Patriarchi T, Koval OM, Anderson ME, He K, Lee HK, Hell JW. β_2-Adrenergic receptor supports prolonged theta tetanus-induced LTP. *J Neurophysiol* 107: 2703–2712, 2012. First published February 15, 2012; doi:10.1152/jn.00374.2011.—The widespread noradrenergic innervation in the brain promotes arousal and learning by molecular mechanisms that remain largely undefined. Recent work shows that the β_2-adrenergic receptor (β_2AR) is linked to the AMPA-type glutamate receptor subunit GluA1 via stargazin and PSD-95 (Joiner ML, Lise MF, Yuen EY, Kam AY, Zhang M, Hall DD, Malik ZA, Qian H, Chen Y, Ulrich JD, Burette AC, Weinberg RJ, Law PY, El-Husseini A, Yan Z, Hell JW. *EMBO J* 29: 482–495, 2010). We now demonstrate that the β_2AR plays a prominent role in long-term potentiation (LTP) induced by a train of 900 stimuli at 5 Hz (prolonged theta-tetanus-LTP, or PTT-LTP) in the hippocampal CA1 region in mice, which requires simultaneous β-adrenergic stimulation. Although PTT-LTP was impaired in hippocampal slices from β_1AR and β_2AR knockout (KO) mice, only β_2AR-selective stimulation with salbutamol supported this PTT-LTP in wild-type (WT) slices, whereas β_1AR-selective stimulation with dobutamine (+ prazosin) did not. Furthermore, only the β_2AR-selective antagonist ICI-118551 and not the β_1AR-selective antagonist CGP-20712 inhibited PTT-LTP and phosphorylation of GluA1 on its PKA site S845 in WT slices. Our analysis of S845A knockin (KI) mice indicates that this phosphorylation is relevant for PTT-LTP. These results identify the β_2AR-S845 signaling pathway as a prominent regulator of synaptic plasticity.

beta-adrenergic signaling; postsynaptic signaling; α-amino-3-hydroxy-5-methylisoxazole propionic acid receptors; protein kinase A

NOREPINEPHRINE (NE) is released throughout the brain in a diffuse manner and supports arousal and learning in novel and emotionally charged situations (Berman and Dudai 2001; Cahill et al. 1994; Hu et al. 2007a; Minzenberg et al. 2008; Nielson and Jensen 1994; Strange and Dolan 2004; Strange et al. 2003). NE acts on the β_1 adrenergic receptor (AR) and the β_2AR to stimulate the trimeric protein G_s, adenylyl cyclase (AC), and, via cAMP, ultimately PKA. β-Adrenergic stimulation promotes various forms of long-term potentiation (LTP) in dentate gyrus and CA1 of the hippocampus (Gelinas and Nguyen 2005; Gelinas et al. 2007; Lin et al. 2003; Thomas et al. 1996; Walling and Harley 2004), including LTP following prolonged (90–180 s) θ-rhythm stimulation (Gelinas and Nguyen 2005; Hu et al. 2007a; Katsuki et al. 1997; Thomas et al. 1996), which we call "prolonged theta-tetanus-LTP," or PTT-LTP. The θ-rhythm (5–12 Hz) is a prominent activity pattern of the hippocampus, suggesting that PTT-LTP is an important form of synaptic plasticity (Mizuseki et al. 2009). The strict dependence of PTT-LTP on β-adrenergic stimulation

makes it fundamentally different from the more standard LTP induced by tetani of 50–100 Hz or theta-burst stimulations (TBS), which do not strictly require PKA. However, it is unclear whether PTT-LTP is mediated by the β_1AR, the β_2AR, or both. This question is important because the β_1AR and the β_2AR might participate in different signaling complexes and pathways or regulate common pathways with variant potency or efficacy.

The β_2AR is enriched in dendritic spines and associated with the AMPA receptor (AMPAR) subunit GluA1 and the L-type Ca^{2+} channel $Ca_v1.2$ (Davare et al. 2001; Joiner et al. 2010; Wang et al. 2010). These signaling complexes also contain G_s, AC, PKA, and the counterbalancing phosphatases PP2A and calcineurin/PP2B (Colledge et al. 2000; Davare et al. 1999, 2000, 2001; Hall et al. 2006, 2007; Joiner et al. 2010; Oliveria et al. 2007; Tavalin et al. 2002; Wang et al. 2010). The β_1AR is not detectable in the $Ca_v1.2$ complexes immunoisolated from heart and brain (Balijepalli et al. 2006) (see Fig. 8K). The β_2AR could thus be selectively linked to the regulation of GluA1 and $Ca_v1.2$ in PTT-LTP.

PKA phosphorylates GluA1 on S845, which is crucial for activity-driven postsynaptic accumulation of GluA1 (Esteban et al. 2003) and increased surface expression of GluA1 (Ehlers 2000; Joiner et al. 2010; Man et al. 2007; Oh et al. 2006; Sun et al. 2005; Swayze et al. 2004). This phosphorylation is also important for various forms of synaptic plasticity (He et al. 2009; Lee et al. 2003, 2010; Seol et al. 2007), including βAR-dependent and spike timing-dependent potentiation in the visual cortex (Seol et al. 2007) and potentially also PTT-LTP in CA1 (Hu et al. 2007a). For these reasons we tested whether the β_2AR is important for PTT-LTP. We present several lines of evidence that demonstrate that PTT-LTP depends on the β_2AR and phosphorylation of GluA1 on S845, whereas acute signaling by the β_1AR is largely dispensable.

MATERIALS AND METHODS

Reagents and antibodies. (−)Isoproterenol bitartrate salt, ICI-118551, and CGP-20712 were from Sigma. One batch of ICI-118551 was from Tocris. The phospho-specific antibody against S845 was raised in rabbits against the synthetic peptide TLPRN(pS)GAGASK (GluA1 residues 840–850; pS = phosphoserine) (see Lu et al. 2007 and also Mammen et al. 1997) and the anti-GluA1 antibody against the peptide MSHSSGMPLGATGL (GluA1 residues 876–889 at the very COOH terminus). The peptides had been attached to bovine serum albumin for immunization, as described earlier (Davare et al. 1999). Horseradish peroxidase (HRP)-coupled protein A was from Bio-Rad. The antibodies against the β_2AR (H-20, lot J0305; Santa Cruz) and GluA1 COOH terminus are described by Joiner et al. (2010), against the α_1-subunit of the L-type Ca^{2+} channel $Ca_v1.2$ (anti-CNC1) by Davare et al. (1999), and against the NMDA receptor

Address for reprint requests and other correspondence: J. W. Hell, Dept. of Pharmacology, Univ. of California, Davis, CA 95616-8636 (e-mail: jwhell @ucdavis.edu).
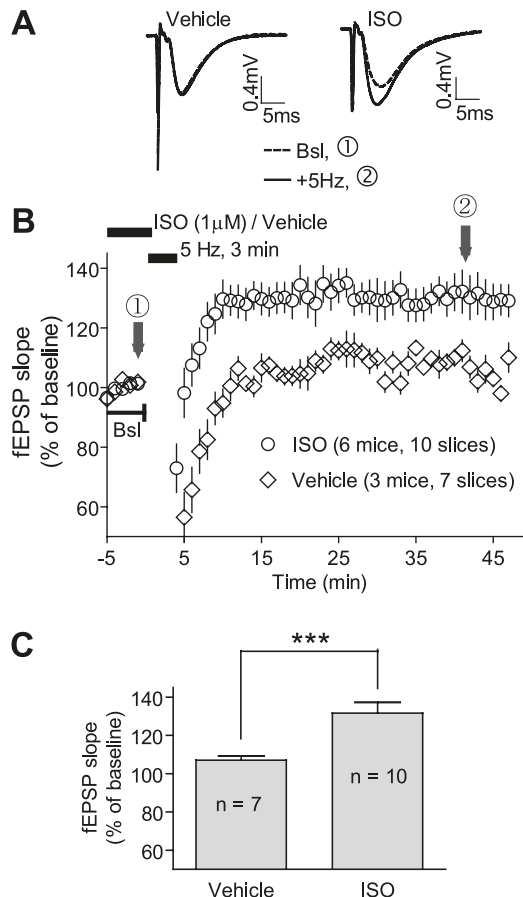
Fig. 1. Isoproterenol (Iso)-dependent induction of prolonged theta-tetanus long-term potentiation (PTT-LTP) by a 5-Hz/3-min tetanus. *A*: examples of field excitatory postsynaptic potentials (fEPSPs) before [baseline (Bsl), dashed lines] and after (solid lines) a 3-min-long 5-Hz tetanus. Graphed are averages of 10 consecutive fEPSPs recorded at the times indicated by arrows in *B*. *B*: time courses of fEPSPs before and after the tetanus (lower bar on *top*). Shown are averages of initial slopes of fEPSP starting after 10 min of onset of perfusion with vehicle (water) and Iso (1 μM) when responses had stabilized. *C*: summary data of PTT-LTP. Baseline corresponding to 100% is the average of fEPSP initial slopes from each individual experiment during the 5 min immediately preceding the tetanus for each experiment. With Iso the potentiation induced by the tetanus was 32 ± 6% above baseline (average of all fEPSP initial slopes between 15 and 45 min after tetanus). In vehicle control, that value was 7 ± 2%. Compared with the baseline and vehicle control, the tetanus significantly increased fEPSP in the presence of Iso (***$P < 0.0001$, 1-way ANOVA).

(NMDAR) subunits GluN1, 2A, and 2B by Leonard and Hell (1997). The polyclonal rabbit antibody against β_1AR (V-19, lot K1209) and the monoclonal mouse antibody against tubulin (32293) were from Santa Cruz. The polyclonal rabbit antibody against synapsin was from Synaptic Systems (106002). The monoclonal mouse antibodies against Shank (N23B/49) and PSD-95 (K28/43) were from Neuro-MAB. ECL and ECL plus reagents were from Amersham. Other reagents were from common commercial suppliers and of standard quality.

Animals. All animal procedures followed National Institutes of Health guidelines and had been approved by the Institutional Animal Care and Use Committees at the University of Iowa, UC Davis, and University of Maryland. Adult New Zealand White rabbits originated from Harlan and C57BL/6 mice from Taconic Farms. The S845A knockin (KI) mice were as previously described (He et al. 2009; Lee et al. 2010; Seol et al. 2007). β_1AR knockout (KO) and β_2AR KO mice were from homozygous breeders in a C57BL/6 background through several backcrossings and generously provided by Dr. B.

Kobilka (Stanford University) (Devic et al. 2001). Mice were 8–16 wk old when used for experiments.

Brain slice preparation and treatment and general immunoblotting. Mice were decapitated, and brains were put into ice-cold artificial cerebrospinal fluid (ACSF). ACSF consisted of (in mM) 127 NaCl, 26 NaHCO$_3$, 1.2 KH$_2$PO$_4$, 1.9 KCl, 2.2 CaCl$_2$, 1 MgSO$_4$, and 10 D-glucose and was oxygenated with 95% O$_2$-5% CO$_2$ (final pH 7.3). About one-third of each brain was trimmed off at the rostral and caudal ends before 350-μm-thick slices were cut with a vibratome (Leica VT 1000A). Slices were maintained in oxygenated ACSF for 1 h at 30°C and then either used for biochemical experiments or kept for 1–5 h at 24°C before being used for electrophysiological analysis.

For biochemical experiments, slices were treated with vehicle, isoproterenol (Iso; 1 μM), ICI-118551 (40–200 nM), and CGP-20712 (500 nM) for 15 min. They were extracted with 1% Triton X-100 in (in mM) 150 NaCl, 10 EDTA, 10 EGTA, 10 Tris·HCl, pH 7.4, containing the protease inhibitors leupeptin (10 μg/ml), aprotinin (10 μg/ml), pepstatin A (1 μM), and phenylmethylsulfonyl fluoride (PMSF, 200 μM) and the phosphatase inhibitor microcystin-LR (2 μM). After ultracentrifugation (30 min, ~250,000 × g) GluA1 was immunoprecipitated, followed by immunoblotting with phospho-specific antibodies against S831 and reprobing with anti-phospho-S845 and ultimately anti-GluA1 for total GluA1 levels (Leonard and Hell 1997; Leonard et al. 1999). To determine levels of various synaptic proteins in β_1AR and β_2AR KO versus wild-type (WT) mice, forebrains were directly extracted with SDS sample buffer. Several exposures of increasing length were made to ascertain that signals were in the linear range (Davare and Hell 2003; Hall et al. 2006). Density values of film signals were corrected for any variation loaded and normalized to control treatment.

Field excitatory postsynaptic potential recording. Brain slices were transferred to the recording chamber and perfused (2 ml/min) at 30°C with ACSF saturated with 95% O$_2$-5% CO$_2$ (final pH 7.3). Field excitatory postsynaptic potentials (fEPSPs) in the hippocampal CA1 region were evoked every 15 s by stimulating the Schaffer collateral
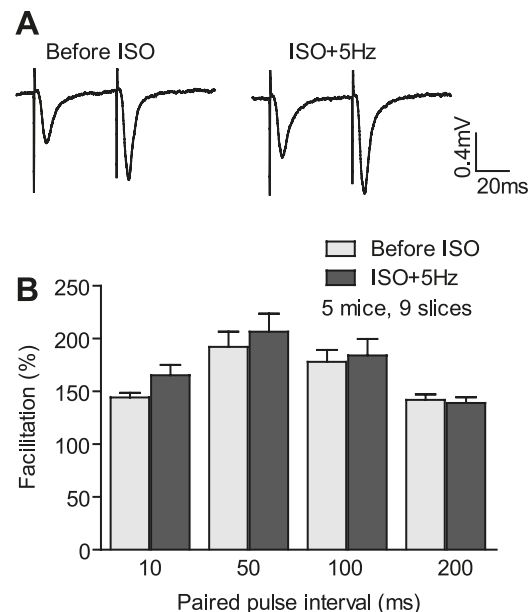

Fig. 2. Paired-pulse facilitation (PPF) was not significantly changed upon PTT-LTP. *A*: averages of 10 consecutive sample traces with interpulse intervals of 50 ms before and after perfusion with Iso and stimulation with 5 Hz for 3 min. *B*: summary graph of the ratios of second to first pulse response for increasing interval lengths. The first pulse was set in each individual recording to equal 100%. None of the ratios before Iso and after tetanization with Iso present was significantly different (*t*-test, $P > 0.05$; 9 slices from 5 mice). PPF measurements after Iso + 5 Hz were taken starting 45 min after the 5-Hz tetanus.

pathway with a bipolar tungsten electrode and recorded with a glass electrode filled with ACSF. Signals were amplified with an Axopatch 2B amplifier, digitized with a Digidata 1320A, and recorded with Clampex 9 (Molecular Devices). The test stimulus strength was set to result in 50% of maximal response. PTT-LTP was induced by a train of pulses of a frequency of 5 Hz lasting 3 min. The baseline was determined by the average of fEPSP initial slopes from the 5-min period immediately before the tetanus. The level of LTP was determined by the average of fEPSP initial slopes from the 30-min period between 15 and 45 min after the tetanus.

For electrophysiological experiments with S845A KI mice and their litter-matched controls, we used dissection buffer (composition in mM: 212.7 sucrose, 2.6 KCl, 1.23 NaH_2PO_4, 26 $NaHCO_3$, 10 dextrose, 3 $MgCl_2$, and 1 $CaCl_2$, saturated with 5% CO_2-95% O_2) for slicing and ACSF (in mM: 124 NaCl, 5 KCl, 1.25 NaH_2PO_4, 26 $NaHCO_3$, 10 dextrose, 1.5 $MgCl_2$, and 2.5 $CaCl_2$, saturated with 5% CO_2-95% O_2) for recording of fEPSPs.

Ventricular myocyte isolation. Adult male New Zealand White rabbits (1.5–2 kg) were anesthetized with pentobarbital sodium (50 mg/ml) containing heparin (55 U/ml) through intravenous injection (1 ml/kg). Hearts were excised, perfused retroaortically (Langendorff), and enzymatically digested with a mixture of collagenase (type 2,

Worthington, 250 U/ml), hyaluronidase (Sigma, 0.01%), and protease type XIV (Sigma, 0.0025%) in a modified Tyrode solution (0.1 mM $CaCl_2$, 10 mM 2,3-butanedione monoxime). Dissociated cardiomyocytes were washed three times in Joklik MEM (Sigma) with 1% Pen/Strep and 1× insulin-transferrin-selenium (ITS) (Sigma) with increasing Ca^{2+} concentration (0.25 mM, 0.5 mM, 0.75 mM). Ventricular myocytes were plated on glass coverslips (glass no. 1) coated with Geltrex (Invitrogen, thin layer) and allowed to attach for 1 h. Cells were washed with a culture medium consisting of a 50:50 mix of DMEM and F-10 medium with 1% Pen/Strep and 1× ITS. Attached cardiomyocytes were counted, and the cell density was calculated.

Whole cell patch-clamp recording from ventricular myocytes. Recording electrodes were fabricated from borosilicate glass with tip diameters of 2–3 μm and resistance of 2–4 M . Electrode pipettes were filled with recording solution (in mM: 150 Cs-MeSO₃, 5 CsCl, 10 HEPES, 10 EGTA, 1 $MgCl_2$, and 4 MgATP, pH 7.2 adjusted with CsOH). Heart cells were perfused with normal Tyrode solution (in mM: 138 NaCl, 4 KCl, 2 $CaCl_2$, 1 $MgCl_2$, 0.33 NaH_2PO_4, 10 HEPES, and 10 glucose, pH 7.4 adjusted with NaOH) at 35°C. After successful break-in, the perfusing medium was switched to an external recording solution (in mM: 137 N-methyl-ᴅ-glucamine aspartate, 10 glucose, 10
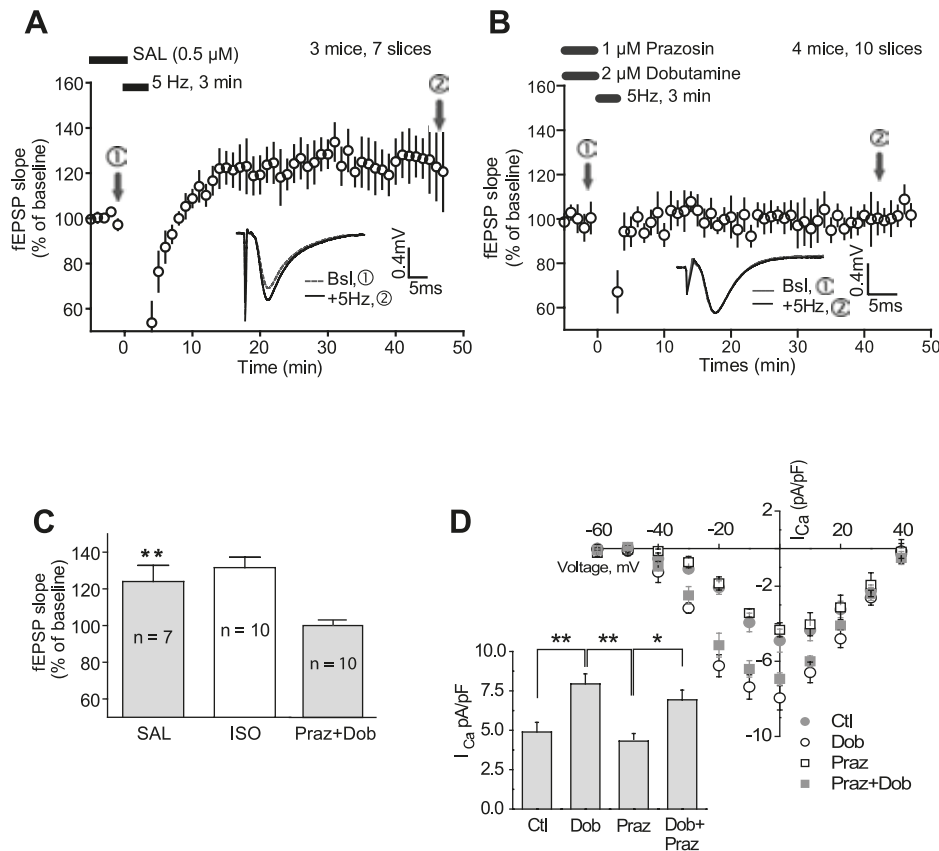

Fig. 3. β₂-adrenergic receptor (β₂AR)- but not β₁AR-selective stimulation facilitates induction of PTT-LTP. *A* and *B*: time courses of fEPSPs before and after the tetanus in the presence of salbutamol (Sal; *A*) or dobutamine + prazosin (*B*). Shown are averages of initial slopes of fEPSP starting after 10 min of onset of perfusion with drugs. *Insets*: example of fEPSPs before (dashed line) and after (solid line) PTT-LTP induction. Graphed are averages of 10 consecutive fEPSPs recorded at the indicated times. *C*: summary graphs of PTT-LTP data. The baseline is the average of fEPSP initial slopes from each individual experiment during the 5 min immediately preceding the tetanus and equaled 100%. The potentiation (average of all fEPSP initial slopes between 15 and 45 min after tetanus minus baseline) induced by the tetanus was 24 ± 9% above baseline for Sal. With Sal, the PTT-LTP level was significantly different from baseline (**P < 0.01; 1-way ANOVA, followed by Dunnett's post hoc test for multiple comparisons) but not from interleaved potentiations with Iso present (32 ± 6% increase; from Fig. 1). No potentiation was detectable after perfusion with 2 μM dobutamine (Dob) and 1 μM prazosin (Praz) (100 ± 3%). *D*: dobutamine effectively activates βAR signaling. L-type Ca^{2+} channel-mediated Ca^{2+} currents (I_{Ca}) were recorded from rabbit cardiomyocytes during depolarizing steps from a holding potential of −80 mV to the indicated potentials. Illustrated are current-voltage (*I-V*) plots (*top*) and summary data of peak currents as measured upon depolarization to −10 mV (*bottom*). The average Ca^{2+} current was 4.79 ± 0.61 pA/pF (mean ± SE; n = 4) in the control group, 7.71 ± 0.52 pA/pF (n = 4) with dobutamine (2 μM), 4.31 ± 0.37 pA/pF (n = 4) with prazosin (1 μM), and 6.93 ± 0.42 pA/pF (n = 4) with dobutamine + prazosin. Stimulation with dobutamine was significant with and without prazosin (1-way ANOVA test, Tukey posttest, *P < 0.05, **P < 0.01).

HEPES, 1.8 CaCl₂, 0.5 MgCl₂, and 25 CsCl, pH 7.4 adjusted with *N*-methyl-D-glucamine aspartate). Whole cell Ca^{2+} currents were recorded with an Axon 200B patch-clamp amplifier (CV-203BU head stage) and digitized with a Digidata 1320A. Experimental control, data acquisition, and data analysis were accomplished with pCLAMP 8.0 (Axon Instruments). Recordings were only obtained from Ca^{2+}-tolerant, rod-shaped ventricular cells. Data traces were acquired at a repetition interval of 2 s from −70 to +60 mV at −80 mV holding potential.

Statistical analysis. Raw data were analyzed with Clampfit 9 software (Molecular Devices). Statistical analysis was performed with Prism 5 (GraphPad software, San Diego, CA). Results are presented as means ± SE. Statistical significance was determined by *t*-test or one-way ANOVA ($P < 0.05$).

RESULTS

Postsynaptic expression of PTT-LTP. To induce PTT-LTP, we applied 3-min-long θ-rhythm stimulations (5 Hz) to the Schaffer collateral pathway and recorded fEPSPs in CA1 stratum radiatum in slices from WT mice in the presence and absence of the β-adrenergic agonist Iso. Summary data show that PTT-LTP was reliably (10 of 10 slices) induced in the presence but not the absence of Iso (Fig. 1). Although this dependence of PTT-LTP on β-adrenergic stimulation is well established (Gelinas and Nguyen 2005; Hu et al. 2007a; Katsuki et al. 1997; Thomas et al. 1996) and postsynaptic complex spike bursting is critical for PTT-LTP (Thomas et al. 1998), whether its expression is actually postsynaptic has not been tested by paired-pulse facilitation (PPF). We analyzed PPF in several slice recordings after the 5-Hz, 180-s tetanus had been administered with and without Iso. There was no significant difference between these two conditions, with interpulse intervals reaching from 10 to 200 ms (Fig. 2). These results indicate that expression of PTT-LTP is likely not due to presynaptic but rather postsynaptic changes.

PTT-LTP is supported by selective β₂AR but not β₁AR stimulation. Salbutamol (Sal; also known as albuterol) is a selective β₂AR agonist (Hoffmann et al. 2004). To test whether activation of the β₂AR is sufficient for PTT-LTP, slices were pretreated with Sal before the induction of PTT-LTP. The
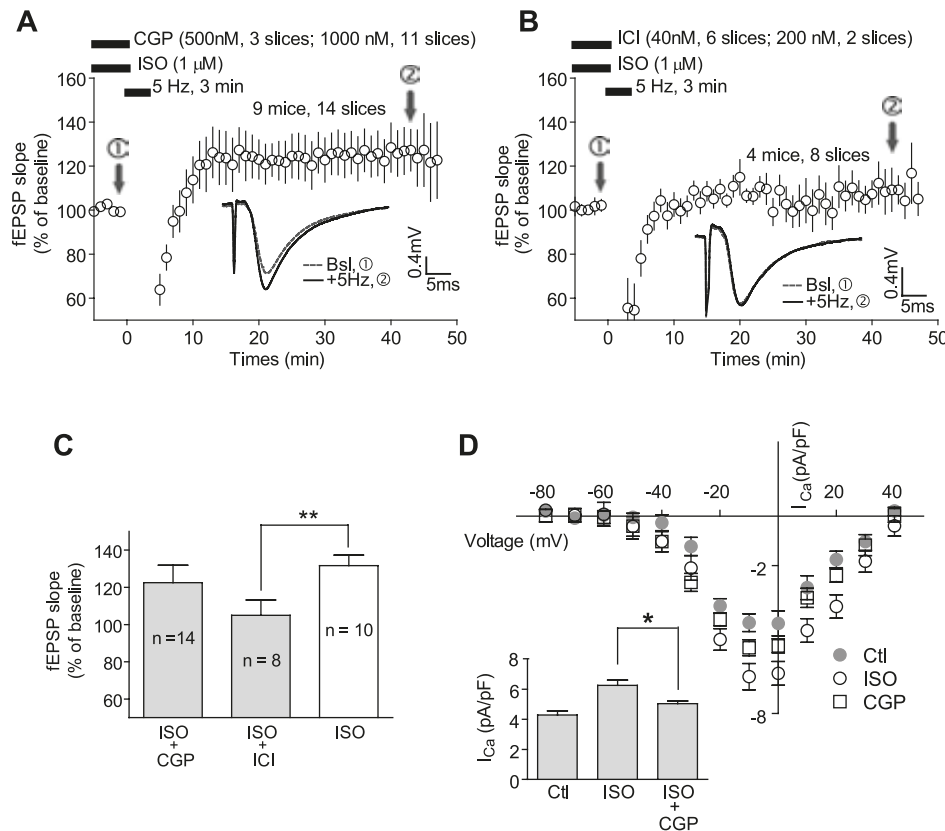

Fig. 4. Induction of PTT-LTP is blocked by a selective β₂AR but not β₁AR antagonist. *A* and *B*: time courses of fEPSPs before and after the tetanus (lower bar) in the presence of Iso (1 μM) + CGP-20712 (*A*) or ICI-118551 (*B*). Shown are averages of initial slopes of fEPSP starting after 10 min of onset of perfusion with Iso + antagonist. *Insets*: example of fEPSPs before (dashed lines) and after (solid lines) PTT-LTP induction. Graphed are averages of 10 consecutive fEPSPs recorded at the indicated times. Because the different antagonist concentrations (initially 500 nM vs. later 1,000 nM CGP-20712 in *A* and initially 200 nM vs. later 40 nM ICI-118551 in *B*) did not result in any obvious differential outcome, all results for each antagonist were combined for statistical analysis. Two different batches of ICI-118551 (1 from Sigma and 1 from Tocris) were tested at the concentration of 40 nM (3 slices each). *C*: summary graph of PTT-LTP recordings. The baseline is the average of fEPSP initial slopes from each individual experiment during the 5 min immediately preceding the tetanus in each experiment and equaled 100%. The potentiation induced by the tetanus was 23 ± 9% for CGP-20712 and 2 ± 5% for ICI-118551 above baseline (average of all fEPSP initial slopes between 15 and 45 min after tetanus). Compared with interleaved Iso-only recordings (32 ± 6% increase; from Fig. 1), the PTT-LTP level was significantly lower for ICI-118551 but not for CGP-20712 (**$P < 0.01$, 1-way ANOVA). *D*: CGP-20712 is an effective β₁AR antagonist. L-type Ca^{2+} channel-mediated Ca^{2+} currents were recorded from rabbit cardiomyocytes during depolarizing steps from a holding potential of −80 mV to the indicated potentials. Illustrated are *I–V* plots (*top*) and summary data of peak currents as measured upon depolarization to −10 mV (*bottom left*). The average Ca^{2+} current was 4.29 ± 0.28 pA/pF (mean ± SE; $n = 4$) in the control group (Ctl), 6.26 ± 0.34 pA/pF ($n = 4$) with Iso (1 μM), and 5.04 ± 0.18 pA/pF ($n = 4$) with Iso + CGP-20712 (1 μM). The inhibitory effect of CGP-20712 on Iso stimulation was significant (1-way ANOVA test, Tukey posttest, *$P < 0.05$).

resulting PTT-LTP was comparable to PTT-LTP induced in the presence of Iso (Fig. 3, *A* and *C*). To test whether selective β_1AR stimulation would also promote PTT-LTP, slices were pretreated with a combination of dobutamine and prazosin. Dobutamine activates the β_1AR and the α_1AR but not the β_2AR or any dopaminergic receptors. Coapplication of the highly selective α_1AR antagonist prazosin allows for selective β_1AR stimulation. Perfusion of slices with a combination of these two drugs did not support induction of PTT-LTP (Fig. 3, *B* and *C*). To ensure that these drugs worked in our hands, we tested their effects on Iso-induced upregulation of Ca^{2+} currents through L-type Ca^{2+} channels in cardiomyocytes, which is mediated by the β_1AR and to a lesser degree by the β_2AR (see, e.g., Balijepalli et al. 2006). Indeed, the same batch of

dobutamine significantly increased Ca^{2+} currents through L-type Ca^{2+} channels in rabbit cardiomyocytes (Fig. 3*D*), thus proving its activity. These results indicate that activation of the β_2AR but not the β_1AR is sufficient for induction of PTT-LTP.

PTT-LTP is blocked by β_2AR antagonist ICI-118551 but not β_1AR antagonist CGP-20712. To further test the role of β_1AR versus β_2AR in PTT-LTP pharmacologically, CGP-20712 or ICI-118551 was coapplied with Iso before the 5-Hz/3-min tetani (Fig. 4). CGP-20712 is a highly selective β_1AR antagonist and ICI-118551 a highly selective β_2AR antagonist (Hoffmann et al. 2004). We initially used 500 nM CGP-20712 in three slices, without any obvious effect on the magnitude of the PTT-LTP (Fig. 4, *A* and *C*). As expected, 500 nM CGP-20712 using the same stock solution reduced the Iso-induced upregulation of L-type currents in cardiomyocytes by ~65%, with the remaining upregulation being due to β_2AR signaling (Fig. 4*D*). To further ascertain the lack of impact of β_1AR blockage on PTT-LTP, we increased the CGP-20712 concentration to 1 μM in subsequent experiments, again without observing any significant inhibition (Fig. 4, *A* and *C*).

On the other hand, initial experiments with 200 nM ICI-118551 resulted in a complete block of PTT-LTP. To minimize any potential effect on β_1AR, we then reduced its concentration to 40 nM in subsequent tests, which also blocked the induction of PTT-LTP (Fig. 4, *B* and *C*). These results indicate that signaling by the β_2AR but not the β_1AR is required for PTT-LTP and support a central role of the β_2AR in this form of LTP under our conditions in our C57BL/6 mice.

PTT-LTP is impaired in GluA1 S845A KI mice. PTT-LTP induced by a 90-s/10-Hz train in the presence of NE, which is comparable to our 180-s/5-Hz Iso protocol, was absent in hippocampal slices from KI mice in which S831 and S845 had been replaced by alanine residues (Hu et al. 2007a). However, it is unclear from this study whether S831, S845, or both are required for PTT-LTP, with S831 being a prominent phosphorylation site for CaMKII and PKC (Mammen et al. 1997; Roche et al. 1996; Tavalin 2008). We used single-site S845A KI mice to evaluate whether PTT-LTP depends on S845. PTT-LTP was reduced by >60% in hippocampal slices from homozygous S845A mice compared with PTT-LTP in littermate control slices (Fig. 5, *A* and *C*). Although there appeared to be a small potentiation by the 180-s/5-Hz tetanus in the KI mice, the
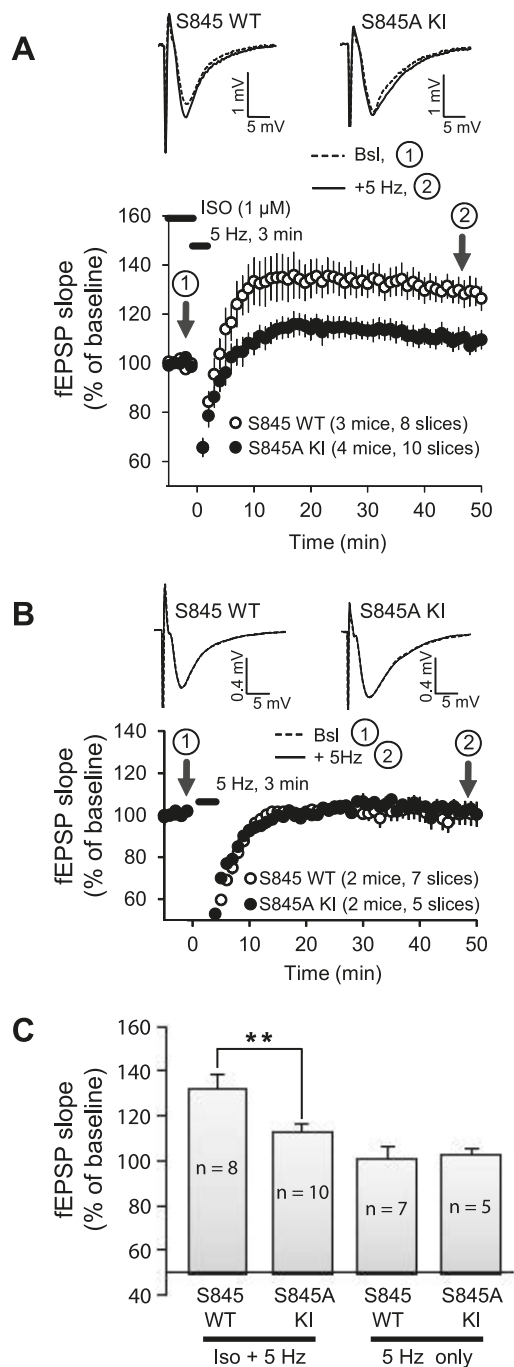

Fig. 5. PTT-LTP is impaired in slices from S845A knockin (KI) mice. *A*, *top*: example of fEPSPs before (dashed lines) and after (solid lines) the tetanus in slices from homozygous S845A KI and litter-matched wild-type (WT) mice. Graphed are averages of 10 consecutive fEPSPs recorded at the times indicated at *bottom*. *Bottom*: time courses of fEPSPs before and after the tetanus (lower bar on *top*) from WT and S845A mice in the presence of Iso. Shown are averages of initial slopes of fEPSP starting after ~15 min of onset of perfusion with Iso (1 μM). *B*: experiments analogous to *A* but in the absence of Iso. *C*: summary graph of PTT-LTP. Baseline corresponding to 100% is the average of the fEPSP initial slopes from each individual experiment during the 5 min immediately preceding the tetanus in each experiment. The potentiation induced by the tetanus with Iso present was 13 ± 4% (paired *t*-test: $P < 0.05$; 10 slices, 4 mice) for S845A KI and 33 ± 6% (paired *t*-test: $P < 0.005$; 8 slices, 3 mice) for WT above baseline (average of all fEPSP initial slopes between 15 and 45 min after tetanus). The potentiation in S845A KI mice was significantly lower than in WT (**$P < 0.01$; 1-way ANOVA, followed by Fisher's protected least significant difference post hoc test for multiple comparisons) and actually was statistically not different from the strength of synaptic transmission before the tetanus and also not different from the lack of potentiation by the tetanus in the absence of Iso.

difference between before versus after the tetanus is statistically not significant. There was no detectable potentiation at all by the tetanus in slices from either WT or S845A KI mice in the absence of Iso (Fig. 5B). However, the modest potentiation observed in the KI mice after the tetanus is statistically not significantly different from the complete lack of potentiation in the KI mice observed upon application of Iso alone, without the tetanus. Thus it appears that S845 phosphorylation is absolutely critical for PTT-LTP. However, a lack of statistical significance in the preceding comparisons does not absolutely exclude that there is no difference and thereby no potentiation in S845A KI mice. Given the tendency to an increase in fEPSP slope after the tetanus with Iso present in S845A mice, even if it does not reach statistical significance, we cannot rule out that a small portion of PTT-LTP is present in S845A KI mice and does not require S845 phosphorylation, with phosphorylation of S831 potentially being able to partially compensate.

Iso-induced S845 phosphorylation mainly depends on β_2AR. As S845 phosphorylation is important for a substantial portion of PTT-LTP (Fig. 5), we further scrutinized a potential role of the β_2AR and also the β_1AR in β-adrenergic regulation of GluA1 in the forebrain and perhaps PTT-LTP by evaluating the sensitivity of Iso-triggered S845 phosphorylation to ICI-118551 and CGP-20712. Acute forebrain slices were treated with and without Iso and ICI-118551. ICI-118551 inhibited Iso-induced phosphorylation of GluA1 on S845 in acute forebrain slices (Fig. 6, A and B). In analogous experiments CGP-20712 showed no effect on Iso-induced phosphorylation of S845 (Fig. 6A). This lack of effect was not due to problems with the potency of CGP-20712 (see Fig. 4D). To test whether unknown side effects of Iso on targets other than βARs could account for a lack of CGP-20712 on S845 phosphorylation, ICI-118551 was coapplied with CGP-20712, which largely blocked Iso-induced phosphorylation (Fig. 6A). The incomplete block of Iso-induced phosphorylation of S845 with ICI-118551 from Sigma in Fig. 6A contrasts the effect of the apparently more effective ICI-118551 from Tocris in Fig. 6B, which not only completely blocked the Iso-induced phosphorylation but also reduced S845 phosphorylation below baseline levels, reflecting that a portion of the basal phosphorylation is due to basal β_2AR activity. To test whether selective β_1AR stimulation could possibly induce S845 phosphorylation without being really necessary, slices were incubated with dobutamine plus prazosin, which did not augment S845 phosphorylation (Fig. 6C). These results indicate that signaling by the β_2AR but not the β_1AR effectively enhances S845 phosphorylation under our conditions in our C57BL/6 mice.

PTT-LTP and PPF are impaired in β_1AR and β_2AR KO mice. Finally, we used β_1AR and β_2AR KO mice to evaluate the effect of complete elimination of either βAR on PTT-LTP and on the phosphorylation of GluA1 on S845 by PKA. The 3-min/5-Hz tetanus in the presence of Iso did not significantly potentiate fEPSPs in slices from β_1AR or β_2AR KO mice (Fig. 7, A–C). However, these results do not establish an acute requirement of either AR during the induction of PTT-LTP, as KO of either AR could lead to developmental changes in molecular mechanisms that regulate synaptic functions. In fact, synaptic transmission at Schaffer collateral-CA1 synapses showed a reduction in PPFs in both KO mice (Fig. 7D). These results indicate alterations in presynaptic glutamate release or postsynaptic AMPAR properties such as desensitization in
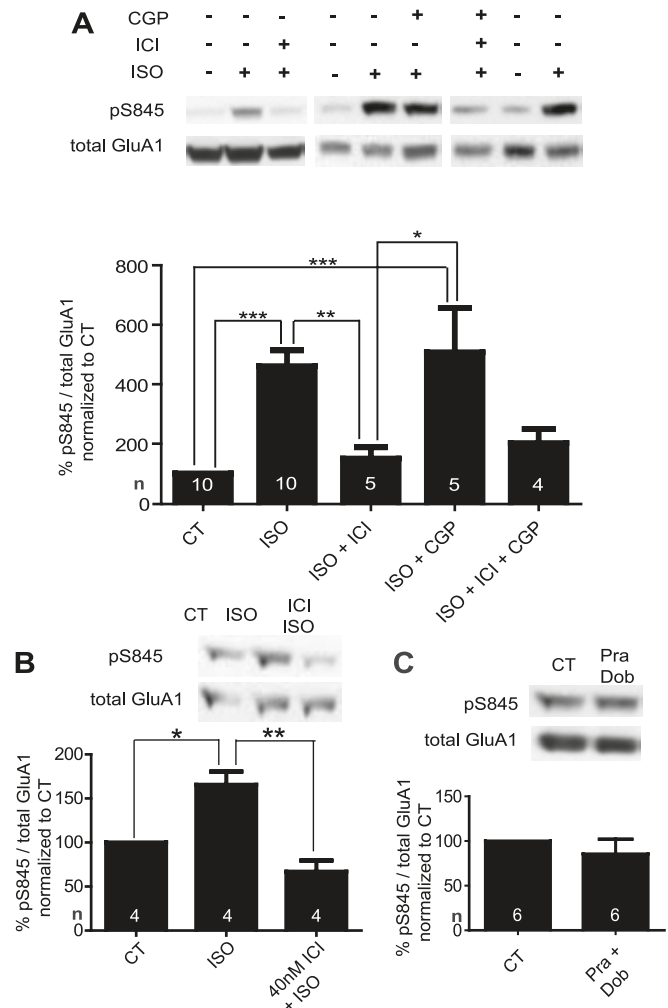

Fig. 6. Iso-induced phosphorylation of GluA1 on S845 is mainly mediated by signaling via β_2AR but not β_1AR. Acute forebrain slices were treated with vehicle (control, CT), 1 μM Iso alone or in combination with 500 nM CGP-20712 (A) and 40 nM ICI-118551 from Sigma (A) or from Tocris (B), or a combination of 2 μM dobutamine (Dob) + 1 μM prazosin (Pra) (C) for 15 min before extraction, clearance by ultracentrifugation, immunoprecipitation of GluA1, and immunoblotting with antibodies against phospho-S845 and subsequently against total GluA1. *Top*: representative sample blots. *Bottom*: quantified immunosignals of phospho (p)S845, which were corrected for variations in total GluA1 signals. Graphed are means $\pm$ SE for various treatments as % of control group (equaling 100%) from a total of 14 independent experiments (*$P < 0.05$, **$P < 0.01$, *** $P < 0.001$; 1-way ANOVA).

both KO mice versus WT mice. Input-output analysis of fEPSPs with increasingly stronger stimulus strengths and thereby presynaptic activation as quantified by the presynaptic fiber volley did not reveal significant differences that would suggest alterations in postsynaptic responses (Fig. 7E). Thus the decrease in PPF in both KO mice indicates alterations in presynaptic functions.

Alterations in synaptic protein content and in Iso-induced phosphorylation of S845 in β_1AR and β_2AR KO mice. To characterize β_1AR and β_2AR KO mice on a molecular level, we quantified total protein content for the AMPAR subunit GluA1, the NMDAR subunits GluN1, 2A, and 2B, the structural postsynaptic proteins PSD-95 and Shank, and the presynaptic protein synaptophysin (Fig. 8, A–I). Most of these proteins showed normal amounts in both KO mice. However, total Shank content is increased in β_1AR and possibly β_2AR KO
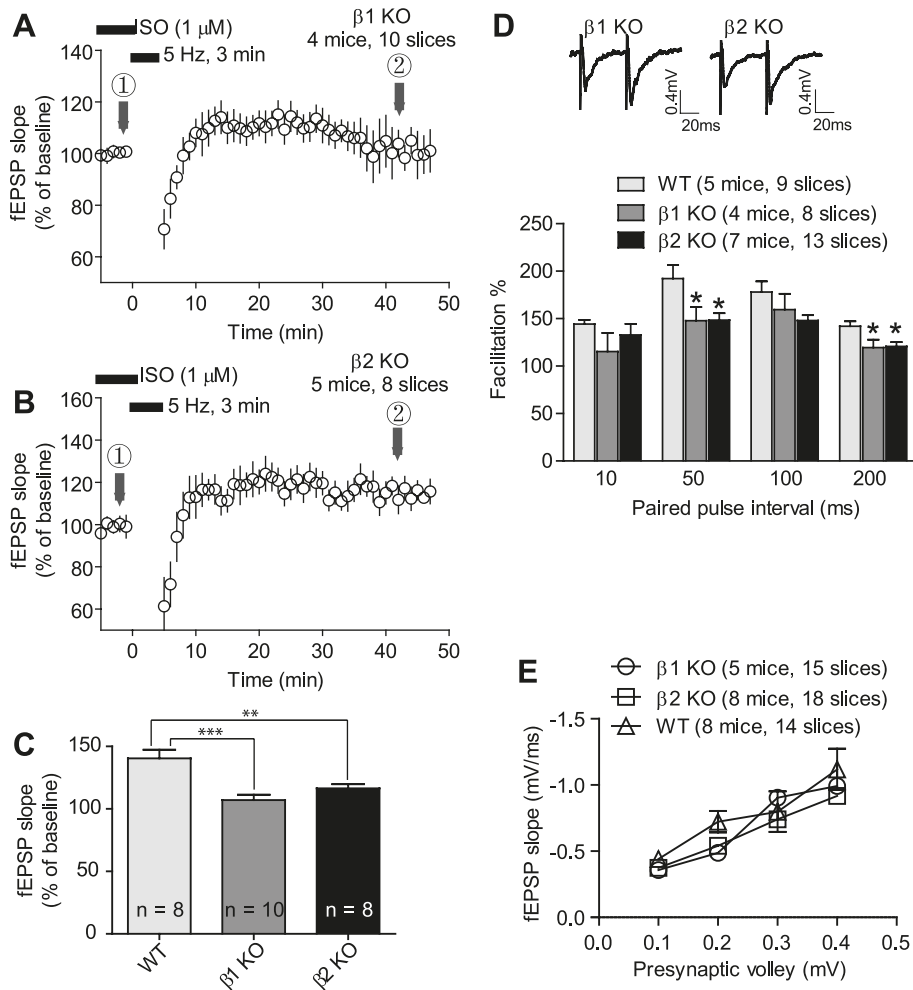
Fig. 7. PTT-LTP as well as presynaptic functions are impaired in slices from both β_1AR knockout (KO) and β_2AR KO mice. *A* and *B*: time courses of fEPSPs before and after the tetanus from β_1AR (*A*) and β_2AR (*B*) KO mice in the presence of Iso. Shown are averages of initial slopes of fEPSP starting after ~15 min of onset of perfusion with Iso. Graphed are averages of 10 consecutive fEPSPs recorded at the indicated times. *C*: summary graph of PTT-LTP. The baseline is the average of the fEPSP initial slopes from each individual experiment during the 5 min immediately preceding the tetanus and equaled 100% for each experiment. The potentiation induced by the tetanus was $7 \pm 4\%$ for β_1AR KO and $17 \pm 4\%$ for β_2AR KO above baseline (average of all fEPSP initial slopes between 15 and 45 min after tetanus). Compared with interleaved WT recordings ($40.4 \pm 6.9\%$ increase), the PTT-LTP levels in both KO mice were significantly lower (**$P < 0.01$, ***$P < 0.0001$; 1-way ANOVA, followed by Dunnett's post hoc test for multiple comparisons). *D*: paired-pulse ratios (PPR) were determined for interpulse intervals of 10–200 ms. Averages of 10 recordings with 50-ms intervals are graphed on *top* and summary data on *bottom*. For 10-ms intervals PPR were $144 \pm 4\%$, $115 \pm 4\%$, and $133 \pm 12\%$ for WT, β_1AR KO, and β_2AR KO, respectively. For 50-, 100-, and 200-ms intervals these values were $192 \pm 14\%$, $148 \pm 15\%$, and $149 \pm 7\%$; $178 \pm 11\%$, $160 \pm 17\%$, and $148 \pm 5\%$; and $142 \pm 5\%$, $119 \pm 8\%$, and $121 \pm 5\%$ (*$P < 0.05$ vs. WT; 1-way ANOVA). *E*: input/output curves for WT, β_1AR KO, and β_2AR KO slices. The averages of the initial slopes of fEPSP are plotted in relation to the amplitude of the presynaptic fiber volley, the latter increasing from 0.1 to 0.4 mV with increasing stimulus strength. Only values from stimulations in which the magnitude of the presynaptic volley was within 10% of the indicated values (*x*-axis) were used for this graph.

mice (Fig. 8*D*) and total GluN2B content in β_2AR KO mice (Fig. 8*F*). The increase in Shank could affect overall postsynaptic organization, and the increase in GluN2B could affect LTP induction by altering Ca^{2+} influx. We also find that the level of basal S845 phosphorylation is increased in β_2AR KO mice (Fig. 8*C*), which could alter perisynaptic AMPAR availability during LTP (see DISCUSSION). Accordingly, both KO mice have some basal alterations in synapse function and expression of postsynaptic protein, which can be expected to affect PTT-LTP and regulation of S845 phosphorylation. In fact, treatment of acutely prepared forebrain slices with Iso for 10 min increased S845 phosphorylation much more in WT than β_2AR KO slices and not at all in β_1AR KO slices (Fig. 8*J*). Accordingly, the presence of both ARs during development or during the actual β-adrenergic stimulation is critical for effective upregulation of S845 phosphorylation in adult hippocampus.

DISCUSSION

The hippocampus shows among other rhythmic activity patterns the θ-rhythm (Mizuseki et al. 2009), and tetani applied for 90–180 s with θ-rhythm frequencies lead to PTT-LTP that depends on β-adrenergic stimulation (Gelinas and Nguyen 2005; Hu et al. 2007a; Katsuki et al. 1997; Thomas et al. 1996). We now demonstrate with a pharmacological approach that the β_2AR is indispensable during the induction phase of PTT-LTP,

whereas the β_1AR is not required during this phase under our conditions. A lack of effect by the β_1AR antagonist CGP-20712 on PTT-LTP cannot be explained by the assumption that the drug might not have been working in our hands because identical batches of stock solutions were successfully tested in parallel experiments on Iso-induced upregulation of L-type channel currents in cardiomyocytes.

At the same time we find that PTT-LTP is strongly impaired in slices from β_1AR and β_2AR KO mice. The impairment in PTT-LTP in β_2AR KO mice is consistent with our pharmacological analysis that indicates that this receptor is required during induction of PTT-LTP. The impairment in PTT-LTP in β_1AR KO mice, however, paired with our pharmacological data that show that the β_1AR is not required during the acute induction phase of PTT-LTP, indicates that the β_1AR is important for the proper development of one or more molecular functions that are required for PTT-LTP but not acutely during PTT-LTP induction. In fact, the decrease in PPF points to alterations in presynaptic functions, and the increase in Shank content could affect postsynaptic organization and signaling in the β_1AR KO mice. Other alterations are conceivable if not to be expected. These changes rather than the lack of the β_1AR could affect PTT-LTP induction during its acute phase. PPF is also decreased in β_2AR KO mice, which show in addition an increase in total GluN2B content. Again these or other, not yet known changes in the β_2AR KO mice could indirectly affect

Fig. 8. Alterations in synaptic protein expression and in Iso-induced phosphorylation of GluA1 on S845 in β_1AR and β_2AR KO mice. A–I: forebrains of WT C57BL/6, β_1AR KO, and β_2AR KO mice were extracted with SDS sample buffer before immunoblotting with the indicated antibodies. Immunosignals were quantified and corrected for variations in total protein loading by dividing by the corresponding relative anti-tubulin signals except for pS845 signals, which were divided by the corresponding relative signals for total GluA1 (C). Graphed are averages ± SE of these ratios from 3 mice for each genotype (*$P < 0.05$, **$P < 0.01$, 1-way ANOVA; $n = 3$ for each genotype). AU, arbitrary units. J: acute forebrain slices from 8- to 16-wk-old WT C57BL/6, β_1AR KO, and β_2AR KO mice were incubated with vehicle or Iso (1 μM) for 10 min before extraction, immunoprecipitation of GluA1, and immunoblotting with antibodies against pS845 (top) and total GluA1 (bottom). Bar diagram illustrates quantified immunosignals of pS845 that were corrected for variations in total GluA1 signals. Graphed are averages ± SE of Iso-treated samples as % of the control, vehicle-treated group (equaling 100%) for each genotype from 4 independent experiments (*$P < 0.05$, **$P < 0.01$, 1-way ANOVA). K: forebrains of WT C57BL/6, β_1AR KO, and β_2AR KO mice were extracted with 1% Triton X-100 before immunoprecipitation (IP) of Ca$_v$1.2, GluA1, or β_1AR vs. control precipitations with nonspecific rabbit IgG and immunoblotting (IB) with antibodies against the very same proteins. The immunoreactive band for the β_1AR was absent in β_1AR KO samples and not detectable in immunoprecipitates of Ca$_v$1.2 or GluA1 from any tissue. Neither Ca$_v$1.2 nor GluA1 was detectable in β_1AR immunoprecipitates except for a minor GluA1 immunoreactivity, which was nonspecific as it was also present in β_1AR KO samples.
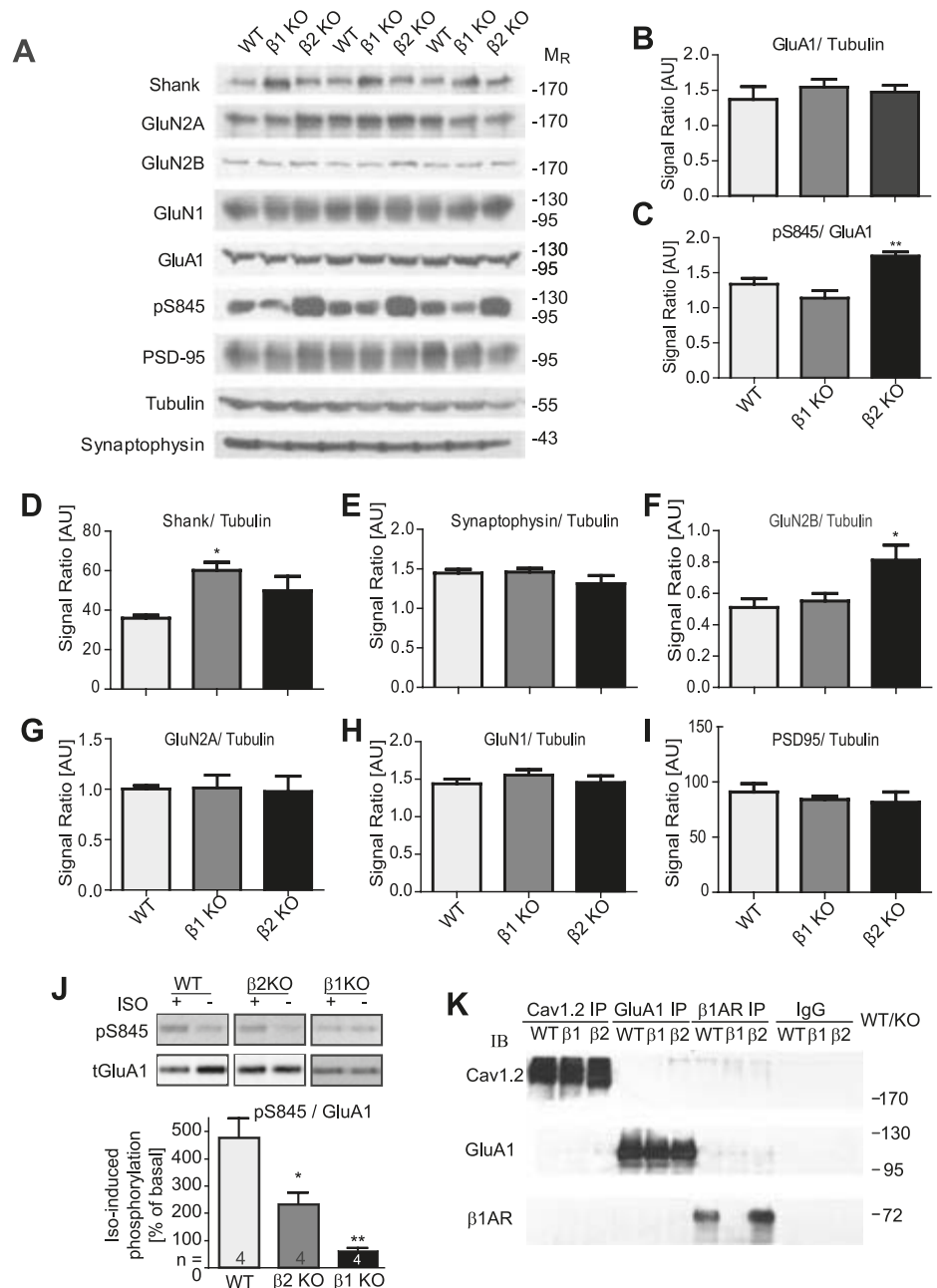
PTT-LTP, but whether or not this is the case our pharmacological analysis shows that the β_2AR is required during the induction phase in WT mice.

Previous work on β_1AR and β_2AR KO mice found that PTT-LTP was absent in the former but normal in the latter (Winder et al. 1999). The differential results in this study versus our study could be due to methodological differences, although most parameters appear to have been comparable. However, our potentiation was 30–40% when it reached 50–100% in the study of Winder et al. (similar to Thomas et al. 1996, but see Gelinas and Nguyen 2005 and Hu et al. 2007a for a more modest 40–50% potentiation; of note, we determined potentiation as the difference between baseline transmission measured after its typically slight but variable 10–20% increase by Iso and transmission 45 min after the tetanus, whereas all the other work includes that 10–20% Iso effect on

baseline). It is possible that the precise electrophysiological setup of Thomas et al. and Winder et al. recruited β_1AR during the acute phase of PTT-LTP induction, whereas in our hands we only recruit β_2AR, thus opening the possibility that under conditions different from ours the β_1AR could mediate a portion of PTT-LTP. In addition, differences in the genetic background could have made the β_1AR more important in the study of Winder et al. than in our studies. Although Winder et al. do not specifically state the genetic background of their KO mice, they obviously used earlier generations of the β_1AR and β_2AR KO mice, which were originally in the FVL background and had not been backcrossed with C57BL/6, whereas we used the same KO mice after their multiple backcrossings with C57BL/6.

Paralleling this difference, an earlier pharmacological study suggests that the β_1AR but not the β_2AR regulates S845

phosphorylation (Vanhoose and Winder 2003). The differences between this and our study, which indicates that the β_2AR rather than the β_1AR regulates S845 phosphorylation, could, once more, be related to differences in the exact experimental systems, although quite similar. An alternative explanation is that the other study used the β_1-selective blocker betaxolol to test for a role of the β_1AR in S845 phosphorylation. The authors used betaxolol at 10 μM, at which concentration its specificity for β_1AR versus β_2AR is likely lost or at least substantially reduced (see, e.g., Sharif and Xu 2004; Smith and Teitler 1999). Accordingly, its antagonistic effect on Iso-induced S845 phosphorylation could have been due to inhibition of the β_2AR rather than the β_1AR. Also, no evidence was presented that the ICI-118551 used in this other study to block the β_2AR was active. In fact, we observed a lack of effect of one batch of ICI-118551 obtained from Sigma during the course of this work, although several other batches from Sigma worked well (Fig. 6A; see also Joiner et al. 2010), as did a new batch from Tocris (Fig. 6B). A lack of effect of ICI-118551 on Iso-induced S845 phosphorylation in the previous work could thus have been due to loss of its activity. Furthermore, we showed earlier that only those GluA1 subunits in AMPAR complexes that are associated with the β_2AR become phosphorylated on S845 upon Iso treatment, further supporting the model that the β_2AR is the principal βAR in governing GluA1 phosphorylation upon β-adrenergic stimulation (Joiner et al. 2010). However, we do not want to completely discard the possibility that the β_1AR can contribute to S845 phosphorylation under certain conditions that differ from ours.

S845 phosphorylation by PKA fosters GluA1 surface expression due to reduced endocytosis rate and enhanced reinsertion rate (Ehlers 2000; Man et al. 2007). More specifically, S845 phosphorylation augments accumulation of GluA1-containing AMPAR at perisynaptic sites (He et al. 2009). These sites serve as reservoir for AMPAR that can be recruited to postsynaptic sites, thereby enhancing LTP induced by TBS (Oh et al. 2006). Signaling by the β_2AR might thus be important for PTT-LTP at least in part because it supports through S845 phosphorylation accumulation of AMPAR at perisynaptic sites, which in turn fosters recruitment of AMPAR to postsynaptic sites upon additional stimulation. However, signaling by the β_2AR might also affect PTT-LTP and other forms of LTP by other signaling pathways. For instance, it could stimulate phosphorylation of different NMDAR subunits by PKA (Leonard and Hell 1997), which enhances Ca^{2+} permeability and thereby postsynaptic Ca^{2+} influx during LTP induction (Skeberdis et al. 2006). Finally, βARs can also act via ERK/MAPK signaling pathways, which is important for PTT-LTP (Winder et al. 1999) as well as LTP induced by a single 1-s/100-Hz tetanus (Gelinas et al. 2007; Gelinas and Nguyen 2005).

Induction of fear and injection of NE can stimulate phosphorylation of GluA1 on S845 and, to a much more modest degree, on S831 (Hu et al. 2007a). KI mice in which both sites have been mutated to alanine are defective in PTT-LTP and in fear conditioning by a diminutive conditioning paradigm (Hu et al. 2007a). KI mice in which S845 has individually been mutated to alanine abrogate priming of neurons in the visual cortex by Iso for spike time-dependent potentiation (Seol et al. 2007). These findings indicate that S845 phosphorylation plays an important role in spike time-dependent potentiation in the

visual system, which mirrors its role in PTT-LTP in CA1. Interestingly, SS831/845AA double-KI mice show reduced TBS-induced LTP (Lee et al. 2003) but neither S831A nor S845A single-KI mice have this deficit (Lee et al. 2010). These results suggest that the more potent TBS protocol can engage phosphorylation of both S845 and S831 through CaMKII/PKC and PKA, respectively, with either being sufficient for full expression of TBS-LTP. In contrast, our findings indicate that S831 phosphorylation is not sufficient and S845 is required for most if not all of PTT-LTP.

Our results identify the β_2AR as a critical component in the signaling events that underlie induction of PTT-LTP. This signaling pathway could thus be important for mediating noradrenergic effects in the brain, including augmenting arousal, synaptic plasticity, and learning (Berman and Dudai 2001; Cahill et al. 1994; Hu et al. 2007b; Nielson and Jensen 1994; Strange and Dolan 2004; Strange et al. 2003). Our findings also highlight the importance of noradrenergic innervation of the hippocampus and other forebrain areas, which is usually eliminated in acute slice experiments but must not be ignored.

DISCLOSURES

No conflicts of interest, financial or otherwise, are declared by the author(s).

AUTHOR CONTRIBUTIONS

Author contributions: H.Q., L.M., M.Z., O.M.K., M.E.A., K.H., H.K.L., and J.W.H. conception and design of research; H.Q., L.M., M.Z., M.N., T.P., O.M.K., K.H., and H.K.L. performed experiments; H.Q., L.M., M.Z., M.N., T.P., O.M.K., K.H., H.K.L., and J.W.H. analyzed data; H.Q., L.M., M.Z., O.M.K., M.E.A., K.H., H.K.L., and J.W.H. interpreted results of experiments; H.Q., L.M., T.P., O.M.K., K.H., H.K.L., and J.W.H. prepared figures; H.Q. and J.W.H. drafted manuscript; H.Q., L.M., O.M.K., M.E.A., and J.W.H. edited and revised manuscript; H.Q., L.M., and J.W.H. approved final version of manuscript.

REFERENCES

Balijepalli RC, Foell JD, Hall DD, Hell JW, Kamp TJ. Localization of cardiac L-type Ca^{2+} channels to a caveolar macromolecular signaling complex is required for beta$_2$-adrenergic regulation. *Proc Natl Acad Sci USA* 103: 7500–7505, 2006.

Berman DE, Dudai Y. Memory extinction, learning anew, and learning the new: dissociations in the molecular machinery of learning in cortex. *Science* 291: 2417–2419, 2001.

Cahill L, Prins B, Weber M, McGaugh JL. Beta-adrenergic activation and memory for emotional events. *Nature* 371: 702–704, 1994.

Colledge M, Dean RA, Scott GK, Langeberg LK, Huganir RL, Scott JD. Targeting of PKA to glutamate receptors through a MAGUK-AKAP complex. *Neuron* 27: 107–119, 2000.

Davare MA, Avdonin V, Hall DD, Peden EM, Burette A, Weinberg RJ, Horne MC, Hoshi T, Hell JW. A beta$_2$ adrenergic receptor signaling complex assembled with the Ca^{2+} channel Cav1.2. *Science* 293: 98–101, 2001.

Davare MA, Dong F, Rubin CS, Hell JW. The A-kinase anchor protein MAP2B and cAMP-dependent protein kinase are associated with class C L-type calcium channels in neurons. *J Biol Chem* 274: 30280–30287, 1999.

Davare MA, Hell JW. Increased phosphorylation of the neuronal L-type Ca^{2+} channel Ca$_v$1.2 during aging. *Proc Natl Acad Sci USA* 100: 16018–16023, 2003.

Davare MA, Horne MC, Hell JW. Protein phosphatase 2A is associated with class C L-type calcium channels (Ca$_v$1.2) and antagonizes channel phos-

phorylation by cAMP-dependent protein kinase. *J Biol Chem* 275: 39710–39717, 2000.

Devic E, Xiang Y, Gould D, Kobilka B. Beta-adrenergic receptor subtype-specific signaling in cardiac myocytes from beta₁ and beta₂ adrenoceptor knockout mice. *Mol Pharmacol* 60: 577–583, 2001.

Ehlers MD. Reinsertion or degradation of AMPA receptors determined by activity-dependent endocytic sorting. *Neuron* 28: 511–525, 2000.

Esteban JA, Shi SH, Wilson C, Nuriya M, Huganir RL, Malinow R. PKA phosphorylation of AMPA receptor subunits controls synaptic trafficking underlying plasticity. *Nat Neurosci* 6: 136–143, 2003.

Gelinas JN, Nguyen PV. Beta-adrenergic receptor activation facilitates induction of a protein synthesis-dependent late phase of long-term potentiation. *J Neurosci* 25: 3294–3303, 2005.

Gelinas JN, Banko JL, Hou L, Sonenberg N, Weeber EJ, Klann E, Nguyen PV. ERK and mTOR signaling couple beta-adrenergic receptors to translation initiation machinery to gate induction of protein synthesis-dependent long-term potentiation. *J Biol Chem* 282: 27527–27535, 2007.

Hall DD, Davare MA, Shi M, Allen ML, Weisenhaus M, McKnight GS, Hell JW. Critical role of cAMP-dependent protein kinase anchoring to the L-type calcium channel Cav1.2 via A-kinase anchor protein 150 in neurons. *Biochemistry* 46: 1635–1646, 2007.

Hall DD, Feekes JA, Arachchige Don AS, Shi M, Hamid J, Chen L, Strack S, Zamponi GW, Horne MC, Hell JW. Binding of protein phosphatase 2A to the L-type calcium channel Cav1.2 next to Ser1928, its main PKA site, is critical for Ser1928 dephosphorylation. *Biochemistry* 45: 3448–3459, 2006.

He K, Song L, Cummings LW, Goldman J, Huganir RL, Lee HK. Stabilization of Ca²⁺-permeable AMPA receptors at perisynaptic sites by GluR1-S845 phosphorylation. *Proc Natl Acad Sci USA* 106: 20033–20038, 2009.

Hoffmann C, Leitz MR, Oberdorf-Maass S, Lohse MJ, Klotz KN. Comparative pharmacology of human beta-adrenergic receptor subtypes—characterization of stably transfected receptors in CHO cells. *Naunyn Schmiedebergs Arch Pharmacol* 369: 151–159, 2004.

Hu H, Real E, Takamiya K, Kang MG, Ledoux J, Huganir RL, Malinow R. Emotion enhances learning via norepinephrine regulation of AMPA-receptor trafficking. *Cell* 131: 160–173, 2007a.

Hu XD, Huang Q, Yang X, Xia H. Differential regulation of AMPA receptor trafficking by neurabin-targeted synaptic protein phosphatase-1 in synaptic transmission and long-term depression in hippocampus. *J Neurosci* 27: 4674–4686, 2007b.

Joiner ML, Lise MF, Yuen EY, Kam AY, Zhang M, Hall DD, Malik ZA, Qian H, Chen Y, Ulrich JD, Burette AC, Weinberg RJ, Law PY, El-Husseini A, Yan Z, Hell JW. Assembly of a beta₂-adrenergic receptor-GluR1 signalling complex for localized cAMP signalling. *EMBO J* 29: 482–495, 2010.

Katsuki H, Izumi Y, Zorumski CF. Noradrenergic regulation of synaptic plasticity in the hippocampal CA1 region. *J Neurophysiol* 77: 3013–3020, 1997.

Lee HK, Takamiya K, Han JS, Man H, Kim CH, Rumbaugh G, Yu S, Ding L, He C, Petralia RS, Wenthold RJ, Gallagher M, Huganir RL. Phosphorylation of the AMPA receptor GluR1 subunit is required for synaptic plasticity and retention of spatial memory. *Cell* 112: 631–643, 2003.

Lee HK, Takamiya K, He K, Song L, Huganir RL. Specific roles of AMPA receptor subunit GluR1 (GluA1) phosphorylation sites in regulating synaptic plasticity in the CA1 region of hippocampus. *J Neurophysiol* 103: 479–489, 2010.

Leonard AS, Hell JW. Cyclic AMP-dependent protein kinase and protein kinase C phosphorylate *N*-methyl-D-aspartate receptors at different sites. *J Biol Chem* 272: 12107–12115, 1997.

Leonard AS, Lim IA, Hemsworth DE, Horne MC, Hell JW. Calcium/calmodulin-dependent protein kinase II is associated with the *N*-methyl-D-aspartate receptor. *Proc Natl Acad Sci USA* 96: 3239–3244, 1999.

Lin YW, Min MY, Chiu TH, Yang HW. Enhancement of associative long-term potentiation by activation of beta-adrenergic receptors at CA1 synapses in rat hippocampal slices. *J Neurosci* 23: 4173–4181, 2003.

Lu Y, Allen M, Halt AR, Weisenhaus M, Dallapiazza RF, Hall DD, Usachev YM, McKnight GS, Hell JW. Age-dependent requirement of AKAP150-anchored PKA and GluR2-lacking AMPA receptors in LTP. *EMBO J* 26: 4879–4890, 2007.

Mammen AL, Kameyama K, Roche KW, Huganir RL. Phosphorylation of the alpha-amino-3-hydroxy-5-methylisoxazole-4-propionic acid receptor GluR1 subunit by calcium/calmodulin-dependent kinase II. *J Biol Chem* 272: 32528–32533, 1997.

Man HY, Sekine-Aizawa Y, Huganir R. Regulation of alpha-amino-3-hydroxy-5-methyl-4-isoxazolepropionic acid receptor trafficking through

PKA phosphorylation of the Glu receptor 1 subunit. *Proc Natl Acad Sci USA* 104: 3579–3584, 2007.

Minzenberg MJ, Watrous AJ, Yoon JH, Ursu S, Carter CS. Modafinil shifts human locus coeruleus to low-tonic, high-phasic activity during functional MRI. *Science* 322: 1700–1702, 2008.

Mizuseki K, Sirota A, Pastalkova E, Buzsaki G. Theta oscillations provide temporal windows for local circuit computation in the entorhinal-hippocampal loop. *Neuron* 64: 267–280, 2009.

Nielson KA, Jensen RA. Beta-adrenergic receptor antagonist antihypertensive medications impair arousal-induced modulation of working memory in elderly humans. *Behav Neural Biol* 62: 190–200, 1994.

Oh MC, Derkach VA, Guire ES, Soderling TR. Extrasynaptic membrane trafficking regulated by GluR1 serine 845 phosphorylation primes AMPA receptors for long-term potentiation. *J Biol Chem* 281: 752–758, 2006.

Oliveria SF, Dell'acqua ML, Sather WA. AKAP79/150 anchoring of calcineurin controls neuronal L-type Ca²⁺ channel activity and nuclear signaling. *Neuron* 55: 261–275, 2007.

Roche KW, O'Brien RJ, Mammen AL, Bernhardt J, Huganir RL. Characterization of multiple phosphorylation sites on the AMPA receptor GluR1 subunit. *Neuron* 16: 1179–1188, 1996.

Seol GH, Ziburkus J, Huang S, Song L, Kim IT, Takamiya K, Huganir RL, Lee HK, Kirkwood A. Neuromodulators control the polarity of spike-timing-dependent synaptic plasticity. *Neuron* 55: 919–929, 2007.

Sharif NA, Xu SX. Binding affinities of ocular hypotensive beta-blockers levobetaxolol, levobunolol, and timolol at endogenous guinea pig beta-adrenoceptors. *J Ocul Pharmacol Ther* 20: 93–99, 2004.

Skeberdis VA, Chevaleyre V, Lau CG, Goldberg JH, Pettit DL, Suadicani SO, Lin Y, Bennett MV, Yuste R, Castillo PE, Zukin RS. Protein kinase A regulates calcium permeability of NMDA receptors. *Nat Neurosci* 9: 501–510, 2006.

Smith C, Teitler M. Beta-blocker selectivity at cloned human beta 1- and beta 2-adrenergic receptors. *Cardiovasc Drugs Ther* 13: 123–126, 1999.

Strange BA, Dolan RJ. Beta-adrenergic modulation of emotional memory-evoked human amygdala and hippocampal responses. *Proc Natl Acad Sci USA* 101: 11454–11458, 2004.

Strange BA, Hurlemann R, Dolan RJ. An emotion-induced retrograde amnesia in humans is amygdala- and beta-adrenergic-dependent. *Proc Natl Acad Sci USA* 100: 13626–13631, 2003.

Sun X, Zhao Y, Wolf ME. Dopamine receptor stimulation modulates AMPA receptor synaptic insertion in prefrontal cortex neurons. *J Neurosci* 25: 7342–7351, 2005.

Swayze RD, Lise MF, Levinson JN, Phillips A, El-Husseini A. Modulation of dopamine mediated phosphorylation of AMPA receptors by PSD-95 and AKAP79/150. *Neuropharmacology* 47: 764–778, 2004.

Tavalin SJ. AKAP79 selectively enhances protein kinase C regulation of GluR1 at a Ca²⁺-calmodulin-dependent protein kinase II/protein kinase C site. *J Biol Chem* 283: 11445–11452, 2008.

Tavalin SJ, Colledge M, Hell JW, Langeberg LK, Huganir RL, Scott JD. Regulation of GluR1 by the A-kinase anchoring protein 79 (AKAP79) signaling complex shares properties with long-term depression. *J Neurosci* 22: 3044–3051, 2002.

Thomas MJ, Moody TD, Makhinson M, O'Dell TJ. Activity-dependent beta-adrenergic modulation of low frequency stimulation induced LTP in the hippocampal CA1 region. *Neuron* 17: 475–482, 1996.

Thomas MJ, Watabe AM, Moody TD, Makhinson M, O'Dell TJ. Postsynaptic complex spike bursting enables the induction of LTP by theta frequency synaptic stimulation. *J Neurosci* 18: 7118–7126, 1998.

Vanhoose AM, Winder DG. NMDA and beta1-adrenergic receptors differentially signal phosphorylation of glutamate receptor type 1 in area CA1 of hippocampus. *J Neurosci* 23: 5827–5834, 2003.

Walling SG, Harley CW. Locus ceruleus activation initiates delayed synaptic potentiation of perforant path input to the dentate gyrus in awake rats: a novel beta-adrenergic- and protein synthesis-dependent mammalian plasticity mechanism. *J Neurosci* 24: 598–604, 2004.

Wang D, Govindaiah G, Liu R, De Arcangelis V, Cox CL, Xiang YK. Binding of amyloid beta peptide to beta2 adrenergic receptor induces PKA-dependent AMPA receptor hyperactivity. *FASEB J* 24: 3511–3521, 2010.

Winder DG, Martin KC, Muzzio IA, Rohrer D, Chruscinski A, Kobilka B, Kandel ER. ERK plays a regulatory role in induction of LTP by theta frequency stimulation and its modulation by beta-adrenergic receptors. *Neuron* 24: 715–726, 1999.